

# **Civil Engineering Journal**

(E-ISSN: 2476-3055; ISSN: 2676-6957)

Vol. 11, No. 09, September, 2025



# Effect of Incorporating Hematite Powder on Torsional Behavior of High Strength Steel Fiber Reinforced Concrete Members

Mohammed S. Abdulhasan <sup>1</sup>\*0, Aqeel H. Chkheiwer <sup>1</sup>0

<sup>1</sup>Department of Civil Engineering, College of Engineering, University of Basrah, Basrah, Iraq.

Received 26 May 2025; Revised 29 July 2025; Accepted 07 August 2025; Published 01 September 2025

#### **Abstract**

This research aims to investigate the effect of hematite powder on the first cracking and ultimate torsional resistance, crack patterns, and angle of twist of high-strength concrete beams strengthened with steel fibers under pure torsion. The study was carried out in two stages. The first stage consisted of six hollow cross-section beams to determine the best ratio and type of steel fiber that provide the highest torsional resistance. The second stage aimed to find the optimal ratio of hematite powder that can improve the torsional resistance of high-strength steel fiber-reinforced concrete without causing implementation problems. This was achieved by testing six hollow cross-section beams with hematite ratios of 0.5%, 1%, 1.5%, 2.5%, 3.5%, and 5% as cement replacements. The results showed that using hematite powder up to 2.5% as a cement replacement, combined with a 1.5% mix of steel fibers (50% end-hooked and 50% corrugated), increased both the first cracking and ultimate torque, along with a relative increase in the angle of twist. Additionally, it delayed crack development, reduced crack width, and increased the number of cracks at failure.

Keywords: Steel Fiber; Reinforced Concrete; Hematite Powder; Pure Torsion.

# 1. Introduction

A torsional moment, or torque (also referred to as a twisting moment, *T*), is a moment that acts along the longitudinal axis of an element. Due to advancements in building design, this type of load has become increasingly common in recent years, as structures are now designed to be more space-efficient, aesthetic, and economical. In designs where structural members are curved or have irregular shapes, the strength and deformation of the structural elements are influenced by the twisting moment. Examples include spandrel beams, curved beams, eccentrically loaded elements, spiral staircases, and box girders in bridges.

Shearing stresses produced by a torsional moment act on the cross-sectional planes of the members subjected to torsion, extending from the axis to the surface of the member. In members with circular cross-sections, the shearing stresses are maximum at the surface of the bar and decrease linearly to zero at the axis. In members with rectangular cross-sections, the shearing stresses are zero at the axis and reach their maximum at the centers of the outer sides. Around the perimeter of a rectangular member, the shearing stresses on each side range from zero at the corners to a maximum at the midpoints [1].

Shearing stresses, also known as shear flow (q), are caused by the twisting action on the member's cross-section and circulate around its perimeter. The term *shear flow* originates from its resemblance to water flowing in a circular pattern [2]. The volume of shear flow remains constant across the section at any given time. One way to visualize the distribution

<sup>\*</sup> Corresponding author: mohammed.saber@uobasrah.edu.iq





© 2025 by the authors. Licensee C.E.J, Tehran, Iran. This article is an open access article distributed under the terms and conditions of the Creative Commons Attribution (CC-BY) license (http://creativecommons.org/licenses/by/4.0/).

of shearing stress on a member's cross-section is through the soap-film analogy. By cutting a circular hole in a plate, covering it with a soap film, and inflating the membrane, the distribution of shear stresses in a circular member's cross-section can be observed. The shearing stress at each point corresponds to the slope of the membrane, with the direction of the slope's tangent line being perpendicular to the shearing tension. The cross-section of the membrane is parabolic, and its slope increases linearly from zero at the axis to a maximum at the periphery, similar to the stress distribution. When the shear stress distribution in a member with a square cross-section is represented by the slopes of radial lines, it demonstrates that torsion design is typically associated with shear design.

Ritter et al. (1899) [2] derived the formulas for calculating the torsional strength of reinforced concrete members, which were later developed by Rausch et al. (1929) [3]. When a member is subjected to a twisting moment (T), shear stresses are generated on the top and front faces of the member. Under pure torsion loading, the principal compressive stresses are equal to the principal tensile stresses, and the shear stresses are equal to both.

In addition to the transverse and longitudinal reinforcement that enhances the response of concrete after the cracking stage, fiber wires can also be used to improve concrete performance. The ACI Code allows the use of discrete steel fibers at a dosage limit of approximately 1.5% of the total volume [4] to enhance the tensile properties of concrete, as fibers provide greater resistance during the post-cracking tensile stage of fiber-reinforced concrete members. When fibers are added to concrete in low to moderate dosages, the elastic modulus and compressive strength are not significantly affected. The main purpose of adding discontinuous steel fibers to the concrete mixture is to restrain and delay crack development [4, 5, 6]. The primary objective of using fibers is to enhance the tensile load-carrying capacity of concrete, depending on the fiber material.

According to ACI Code 318-08 [4], steel fibers were allowed and approved for the first time to be used as minimum shear reinforcement in beams. Based on flexural material tests, fiber-reinforced concrete has been recognized as suitable for shear resistance. Steel fibers in the concrete matrix are described as a non-conventional reinforcement material that improves the mechanical properties of concrete and controls crack development [7]. Because of their ability to transfer tensile stresses across crack surfaces, steel fibers form a bridge known as *crack bridging*. Mures et al. [8] found that using mixed steel fibers (50% end-hooked and 50% corrugated) improved the torsional strength of both normal and high-strength concrete, while reducing crack width and increasing the number of cracks. However, the steel fiber ratio should not exceed 1.5%, as higher dosages reduce workability.

Hematite powder, also known as *iron powder*, is one of the nanoparticle materials that has been incorporated into cement binders to improve the properties of concrete, such as compressive and tensile strength, as well as other characteristics like porosity, permeability, and workability. Nanoparticle materials have been used to enhance the properties of blended concrete. For example,  $Al_2 O_3$  has been applied to improve compressive strength and workability. It has been shown that cement can be advantageously replaced with nano- $Al_2 O_3$  up to a maximum limit of 2%, with an average particle size of 15 nm [9].

Due to its similarity to hematite powder in characteristics such as high density and specific gravity, hematite can influence the properties of concrete, particularly its tensile and compressive strength. Recent studies have reported that using 2.5% hematite as a cement replacement can improve the compressive and tensile strengths by approximately 21.88% and 26.77%, respectively [10].

Because of the importance of nuclear structures and the need to reduce radiation penetration through them, hematite powder has also been used to decrease radiation transmission through such facilities due to its high density. Studies have shown that the addition of this powder can effectively reduce radiation penetration [11]. However, only a limited number of studies have investigated this area, and no research has yet examined the effect of hematite powder on high-strength steel fiber-reinforced concrete under pure torsion. Therefore, this study aims to investigate this specific effect.

# 1.1. Research Significance

Although there are a few studies related to the effect of hematite powder on the properties of concrete, no research has been conducted on its influence on the torsional behavior of high-strength fiber-reinforced concrete under pure torsion. From this point of view, this study aims to determine the effect of using hematite powder as a cement replacement on the torsional behavior of concrete through an experimental program.

# 2. Experimental Work

Figure 1 presents the flow chart of the experimental work, which was conducted in two stages.

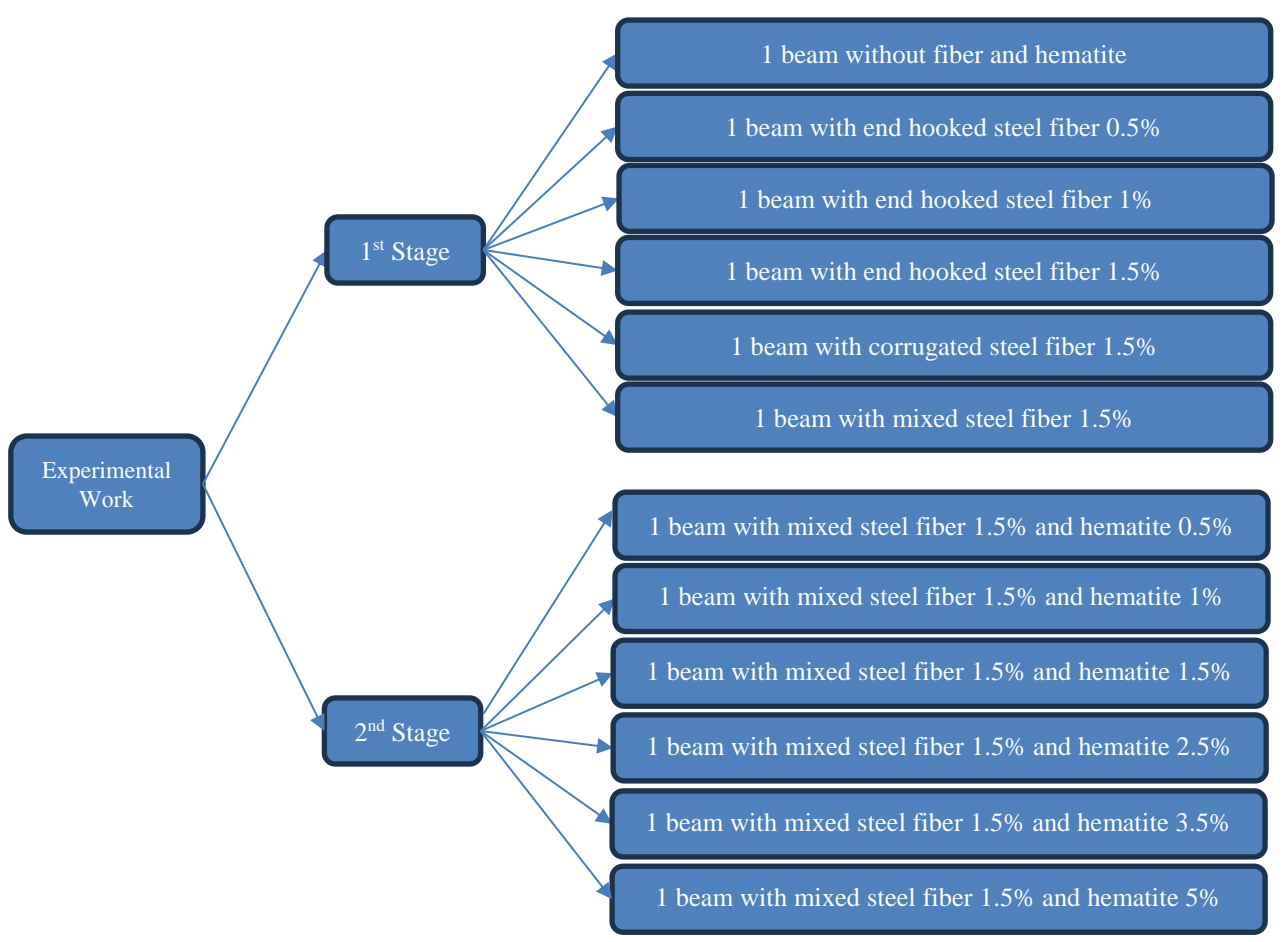


Figure 1. Flow chart of the research methodology

# 2.1. Detail of the Specimens

The experimental work involved casting and testing twelve specimens with hollow cross-sections. The first step was to collect and test the raw materials for the concrete mix, including cement, gravel, sand, water, silica, and additive materials. After testing, a trial mix of plain concrete was prepared to ensure that the compressive strength would not be less than 65 MPa, qualifying it as high-strength concrete. Two types of steel fibers (end-hooked and corrugated) were provided and tested, along with hematite powder (HEMATITE API "Iron Oxide"). Following this step, wooden molds for the specimens were fabricated, as well as a steel frame used during testing to apply pure torsion. This research consisted of two stages, as follows:

*First stage:* Based on previous studies, the optimum percentage of steel fiber that provides the highest torsional strength of concrete with acceptable workability is approximately 1.5% of the concrete volume, using a mix of end-hooked and corrugated steel fibers [8]. In this stage of the study, six concrete beam specimens were prepared to verify this finding. Table 1 presents the details of the first-stage specimens.

Symbol	Shape	Dimensions (mm²)	Shape of Hollow	Dimensions of Hollow (mm²)	Fiber (% of Concrete Volume)	Type of Fiber
F0	Square	200×200	Square	80×80	0	-
F0.5H	Square	200×200	Square	80×80	0.5	End Hooked
F1H	Square	200×200	Square	80×80	1	End Hooked
F1.5H	Square	200×200	Square	80×80	1.5	End Hooked
F1.5C	Square	200×200	Square	80×80	1.5	Corrugated
F1.5M	Square	200×200	Square	80×80	1.5	Mixed

Table 1. Details of First Stage

**Second stage:** This stage was based on the results of the first stage. After verifying the ratio and type of steel fiber that provided the highest torsional resistance, the second stage was prepared to incorporate the effect of hematite powder. Six steel fiber-reinforced concrete beams (H0.5, H1, H1.5, H2.5, H3.5, and H5) were cast with hematite powder ratios of 0.5%, 1%, 1.5%, 2.5%, 3.5%, and 5% as cement replacements, respectively. Table 2 presents the details of the second-stage specimens.

Table 2. Details of Second Stage

Symbol	Shape	Dimensions (mm²)	Shape of Hollow	Dimensions of Hollow (mm²)	Hematite (% of Cement Content)	Fiber (% of Concrete Volume)	Type of Fiber
H0.5	Square	200×200	Square	80×80	0.5	0	Mixed
H1	Square	200×200	Square	80×80	1	0.5	Mixed
H1.5	Square	200×200	Square	80×80	1.5	1	Mixed
H2.5	Square	200×200	Square	80×80	2.5	1.5	Mixed
H3.5	Square	200×200	Square	80×80	3.5	1.5	Mixed
H5	Square	200×200	Square	80×80	5	1.5	Mixed

All specimens from both stages were maintained with the same dimensions: a total length of 1200 mm and a test length of 800 mm. The outer dimensions were  $200 \times 200$  mm, with hollow dimensions of  $80 \times 80$  mm. The reinforcement of all specimens was identical, consisting of four #10 bars as longitudinal reinforcement with a clear concrete cover of 25 mm. Additionally, three closed #12 mm stirrups were fixed at each end to prevent collapse during testing. Figure 2 illustrates the geometry of the specimen.





Figure 2. Geometry of the Specimens

# 2.2. Material of Experimental Work

The materials used in this experimental study were tested in the laboratory of the College of Engineering, Basrah University, and the results were compared with the required specifications.

# Cement

Mabruka Type I Ordinary Portland Cement was used to prepare the concrete mix in this study. Before using the cement, a sample was taken and tested to verify that it met the requirements of ASTM C150 [12] for both physical and chemical properties. The results of the tests are presented in Table 3.

Table 3. Results of Physical Test of Cement

Property	Result	Limit	
Setting Time			
Initial setting time	102	More than 45 min	
Final setting time	218	Less than 600 min	
Compressive Strength (MPa)			
3 days	14.5	More than 8 MPa	
7 days	24.6	More than 15 MPa	

# Coarse Aggregate

The gravel used in this study was obtained from the Al-Zubair field, with a maximum size of 20 mm. Figure 3 illustrates the gradation of the coarse aggregate test conducted in accordance with ASTM C33/C33M-13 [13].

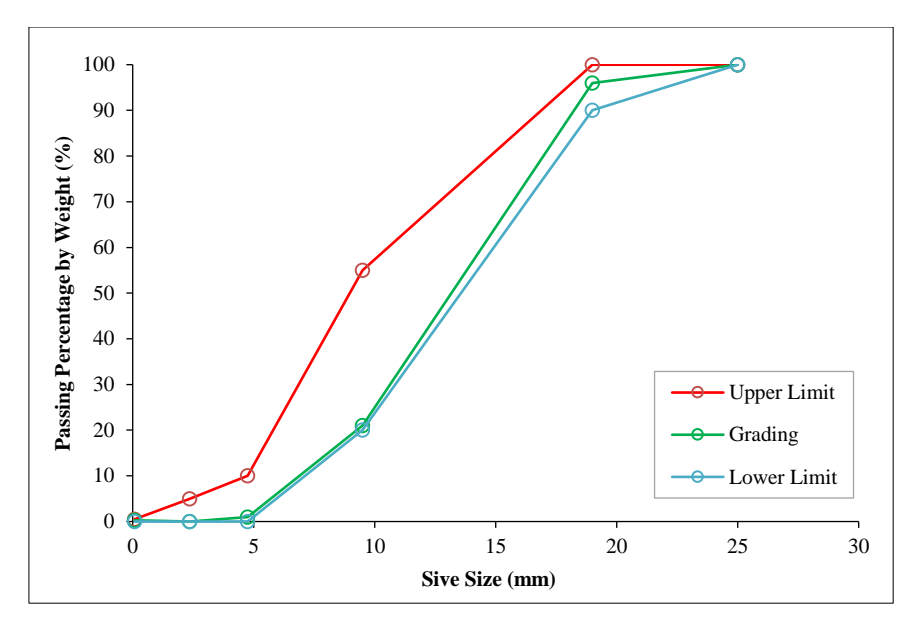


Figure 3. Grading of Coarse Aggregate

# Fine Aggregate

The sand used in this study was obtained from the Al-Zubair natural field, with particle sizes not exceeding 4.75 mm. Figure 4 illustrates the gradation of the fine aggregate test conducted in accordance with ASTM C33/C33M-13 [13].

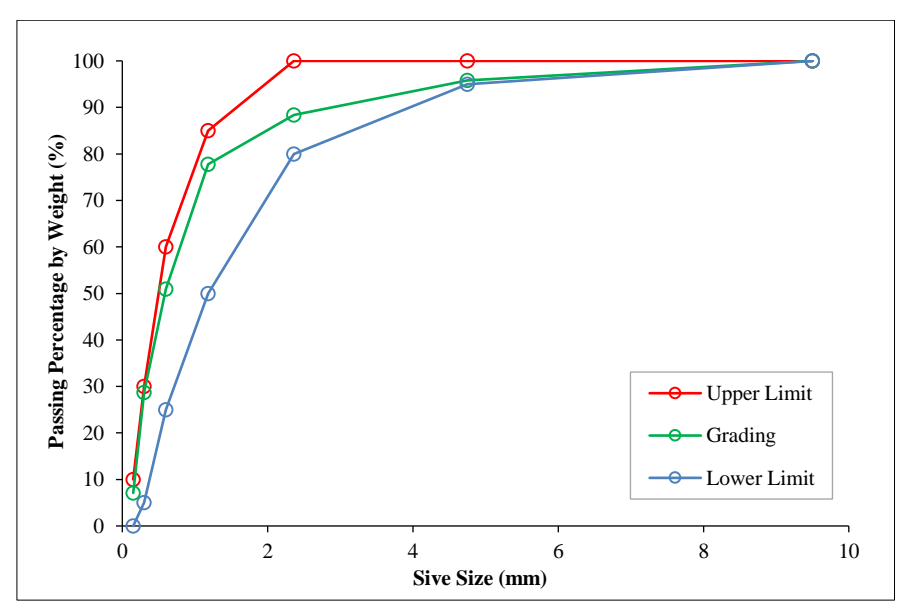


Figure 4. Grading of Fine Aggregate

# Steel Reinforcement

Steel bars with diameters of 12 mm and 10 mm were used in this experimental study for longitudinal reinforcement and stirrups, respectively. A physical test was conducted to verify that the steel met the specifications of ASTM A706/A706M-06 [14], as shown in Table 4.

Table 4. Results of Physical Test of Steel Bars

No.	Standard Diameter (mm)	Yield Stress fy (MPa)	Ultimate Stress fu (MPa)	Bending
1	10	520	690	No crack
2	12	499	670	No crack

In addition to the main concrete materials, additive materials (DCP Hyperplast PC200), silica fume (MegaAdd MS-D), and hematite powder (API) were used. The specifications of these materials were verified based on their original certificates [15, 16].

#### 2.3. Concrete Mix

The concrete mix design was prepared based on the *Concrete Technology* book using the American method of concrete production. High-strength reinforced concrete was targeted to achieve a compressive strength of 65 MPa at 28 days after casting. To achieve this, several experimental trial mixes were conducted to determine the optimum concrete mixture. It was found that the best mix design consisted of 570 kg of cement, 950 kg of gravel (maximum size 20 mm), 700 kg of sand, 50 kg of MegaAdd silica fume, 6 kg of PC additive material, and a water-to-cement ratio (W/C) of 45% per cubic meter of concrete.

#### 2.4. Test Procedure

The universal testing machine was used to apply the load during testing. Figure 5 shows the preparation of the specimen in the testing equipment with all necessary details. The load was applied as a concentrated force at the midpoint of an I-section steel girder, which was connected to the arms fixed at both ends of the specimens at a distance of 0.45 m from the beam's center.





Figure 5. Setup the Test

To measure the twist angle during testing, a Bosch GLM 150 electronic measurement device was used. The devices were fixed on the top surface of the specimens at both ends, as shown in Figure 6.





Figure 6. Measurement of Twist Angle

The loading rate was controlled until cracks appeared on the surface of the specimen. The torsional load and the corresponding twist angle were manually recorded at each load step, which was equal to 0.12 tons, until failure occurred. The load that caused the first torsional crack (first crack load,  $T_{cr}$ ) and the associated twist angle ( $\theta_{cr}$ ) were determined during the test.

# 3. Results and Discussion

# 3.1. Effect of Steel Fiber and Hematite Powder on Structural Behavior and Loading

First Cracking and Ultimate Torque: As shown in the results listed in Table 5, the first cracking and ultimate torque increased with the increasing ratio of end-hooked steel fibers up to 1.5% compared with the control beam (F0). This ratio was used to prepare specimen (F1.5C), but with a different shape of steel fiber—the corrugated type—at the same ratio (1.5%). It was found that the first cracking and ultimate torque increased by 31.3% and 33.33%, respectively, compared to the control specimen (F0). However, when compared with the end-hooked steel fiber at the same ratio (1.5%), it was observed that the end-hooked type provided higher first cracking and ultimate torque than the corrugated steel fiber. Therefore, specimen (F1.5M), which contained a mixed steel fiber composition (50% end-hooked and 50% corrugated), was prepared, cast, and tested. The results showed that this specimen provided the highest first cracking and ultimate torque without any segregation in the concrete and with good workability. The increases in first cracking and ultimate torque were 38.91% and 53.32%, respectively, compared to the control specimen.

Table 5. First	Cracking and	Ultimate Toro	ue (First Stage)

Symbol	Steel Fiber (%)	<i>T<sub>cr</sub></i> (kN.m)	Tu (kN.m)	$\frac{T_u}{T_{cr}}$	$\frac{T_{cr}}{T_{cr}(F0)}$	$\frac{T_u}{T_u(F0)}$	$ heta_{cr}$ (rad/m)	$\theta_U$ (rad/m)
F0	0	4.85	6.18	1.27	-	-	0.0031	0.0136
F0.5H	0.5	5.73	7.5	1.30	1.18	1.21	0.0056	0.0256
F1H	1	6.62	7.94	1.20	1.36	1.28	0.0057	0.0280
F1.5H	1.5	7.50	10.15	1.35	1.54	1.64	0.006	0.0432
F1.5C	1.5	7.06	9.27	1.31	1.45	1.50	0.0058	0.0376
F1.5M	1.5	7.94	13.24	1.66	1.63	2.14	0.0070	0.0448

From this observation, it can be concluded that the best ratio and type of steel fiber is 1.5% of mixed steel fiber, which provides higher torsional strength. This finding is consistent with previous research, such as that of Mures et al. [8]. Based on these results, the second stage was prepared and cast using 1.5% mixed steel fiber. The distribution of the first cracking and ultimate torque is shown in Figure 7.

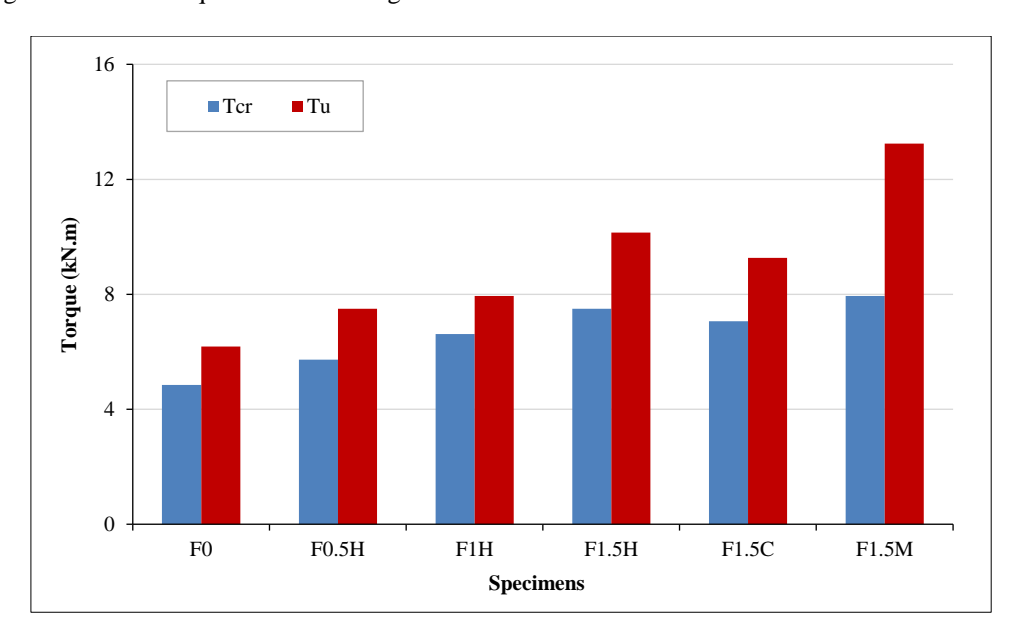


Figure 7. First Cracking and Ultimate Torque of First Stage

The ratio of mixed steel fiber (1.5%) was used in the second stage to investigate the effect of hematite powder as a cement replacement. The specimen (F1.5M) was considered the control specimen for the second stage. As shown in Table 6 and Figure 8, the use of hematite powder resulted in an increase in both the first cracking and ultimate torque. Increasing the hematite powder ratio up to 2.5% led to higher first cracking and ultimate torque values along with an increased angle of twist. The increments were 9.97%, 14.34%, 35.76%, and 41.96% in the first cracking torque, and 3.21%, 11.78%, 21.05%, and 31.82% in the ultimate torque for specimens H0.5, H1, H1.5, and H2.5, respectively. This improvement can be attributed to the increase in compressive and tensile strength of the concrete at this hematite ratio.

Table 6. First Cracking and Ultimate Torque (Second Stage)

Symbol	Hematite Powder (%)	<i>T<sub>cr</sub></i> ( <b>kN.m</b> )	Tu (kN.m)	$\frac{T_u}{T_{cr}}$	$\frac{T_{cr}}{T_{cr}(F1.5M)}$	$\frac{T_u}{T_u(F1.5M)}$	$ heta_{cr}$ (rad/m)	θ <sub>U</sub> (rad/m)
H0.5	0.5	8.82	13.36	1.55	1.11	1.03	0.0071	0.0468
H1	1	9.27	15.009	1.62	1.16	1.13	0.0075	0.0494
H1.5	1.5	12.36	16.77	1.35	1.55	1.26	0.0080	0.0599
H2.5	2.5	13.68	19.42	1.42	1.72	1.46	0.0086	0.0693
H3.5	3.5	13.24	17.21	1.30	1.66	1.29	0.0078	0.063
H5	5	12.36	15.89	1.28	1.55	1.20	0.0070	0.0558

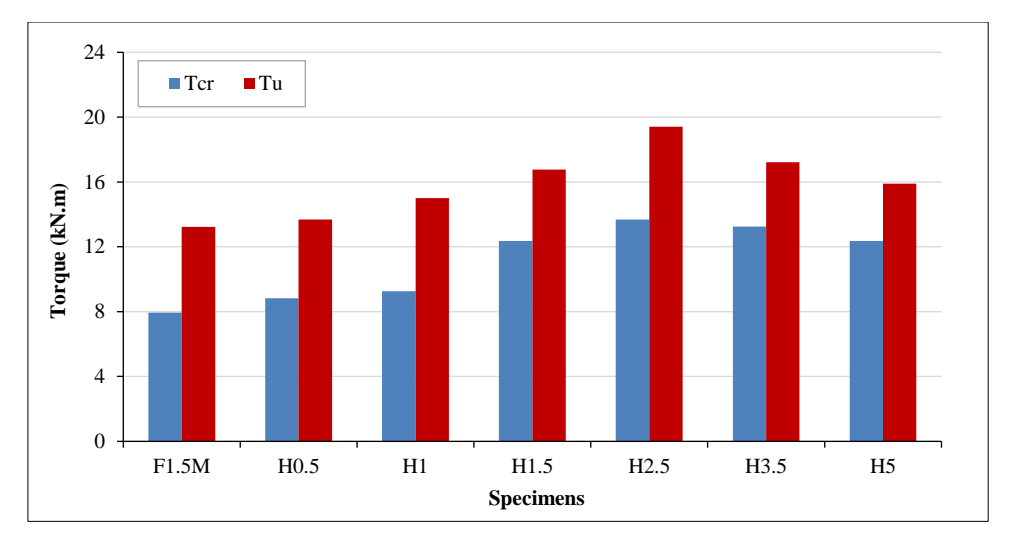


Figure 8. First Cracking and Ultimate Torque of Second Stage

Beyond this ratio, the first cracking and ultimate torque tended to decrease, where the increments were 40.03% and 35.76% in the first cracking torque, and 23.06% and 16.67% in the ultimate torque for specimens H3.5 and H5, respectively, compared with the control specimen F1.5M, although there was still an increase compared with the original control specimen. When the 3.5% and 5% ratios were used, the fresh concrete mix became difficult to handle due to low workability resulting from the high amount of hematite. The main reason for the decrease beyond 2.5% hematite content was the reduction in the compressive and tensile strength of the concrete. Additionally, increasing the hematite ratio as a cement replacement led to a decrease in cement content, which significantly affected the tensile and compressive strength of the concrete. This reduction subsequently influenced the first cracking and ultimate torque, making these higher ratios ineffective and uneconomical.

**Torque and angle of twisting relationship:** As shown in Table 6, the first cracking torque and ultimate torsional strength increased with the addition of hematite powder up to 2.5%. This improvement resulted from enhanced compressive and tensile strength of the concrete. The first cracking resistance mainly depends on the tensile strength of the concrete, while the ultimate torsional resistance depends on the reinforcement and additional materials that improve the concrete's ability to carry load in the post-cracking stage, as well as the contribution of compressive strength.

Incorporating hematite powder into the mixed steel fiber-reinforced concrete further enhanced the torsional behavior. As illustrated in Figures 9 to 13, the torque—twist angle behavior progressed through three distinct stages. In the initial stage, all specimens exhibited a linear response characterized by high torque with minimal twisting angles, indicating similar initial stiffness. The cracking stage followed, marked by crack propagation. The third stage, the post-cracking stage, occurred when each curve reached its maximum torque and then gradually declined, indicating concrete damage and reduced torsional resistance. It is noteworthy that the increase in ultimate torsional strength, along with a significant relative increase in the angle of twist, resulted from the effect of discontinuous mixed steel fibers in the concrete. These fibers acted as bridges across crack paths, restricting and delaying crack propagation, and preventing crack widening under increasing loads [17]. Additionally, replacing part of the cement with hematite powder enhanced both compressive and tensile strength. The nanoparticles of hematite reduced the cement paste's pore volume, improving particle packing density [9], and increased the cohesion between cement, aggregates, and steel fibers.

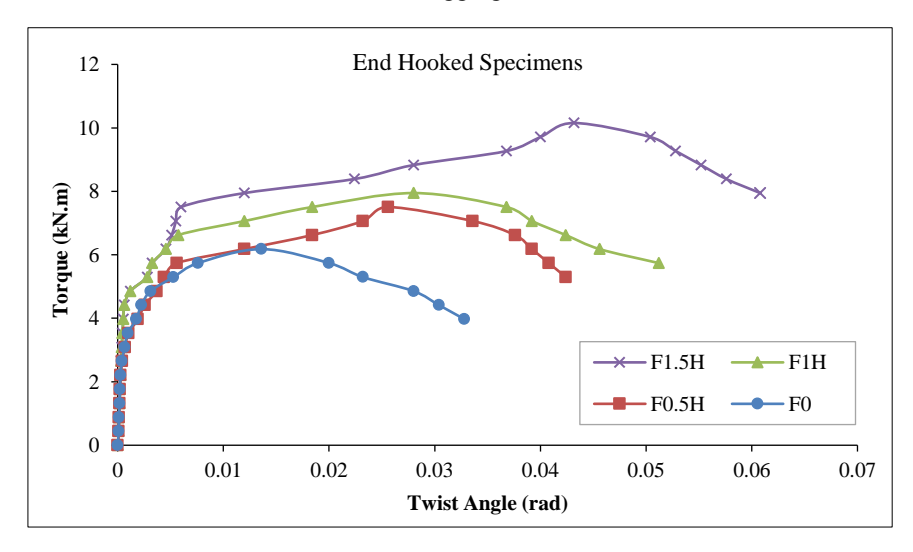


Figure 9. Relationship of Torque-Twist Angle of End Hooked Steel Fiber

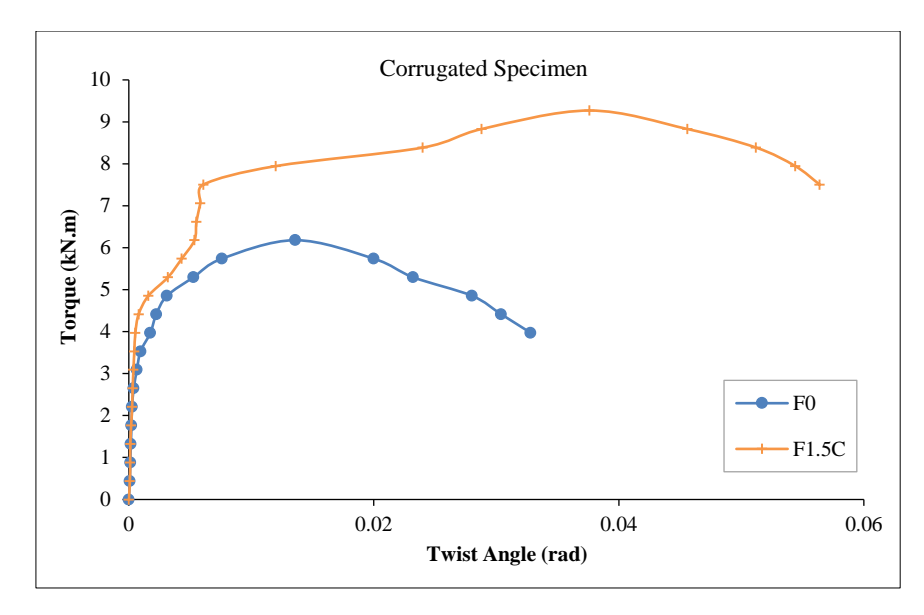


Figure 10. Relationship of Torque-Twist Angle of End Corrugated Steel Fiber

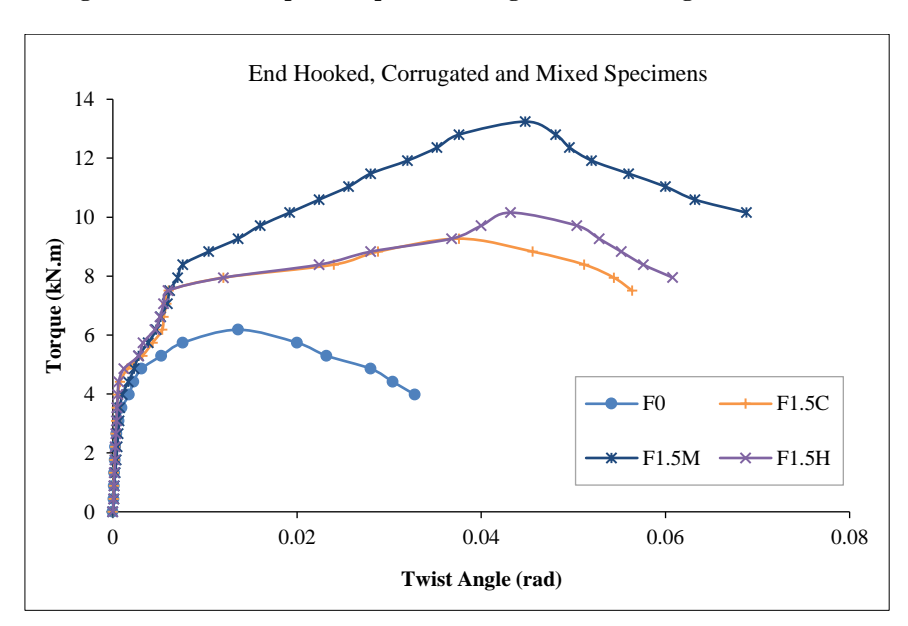


Figure 11. Relationship of Torque-Twist Angle of End Mixed Steel Fiber Compared with End Hooked and Corrugated Steel Fiber

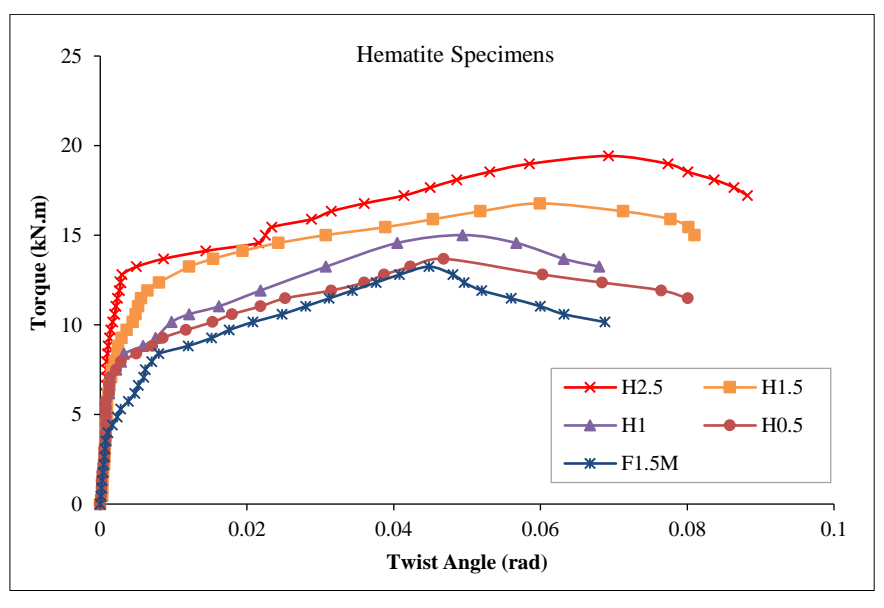


Figure 12. Relationship of Torque-Twist Angle (Hematite Ratio up to 2.5%)

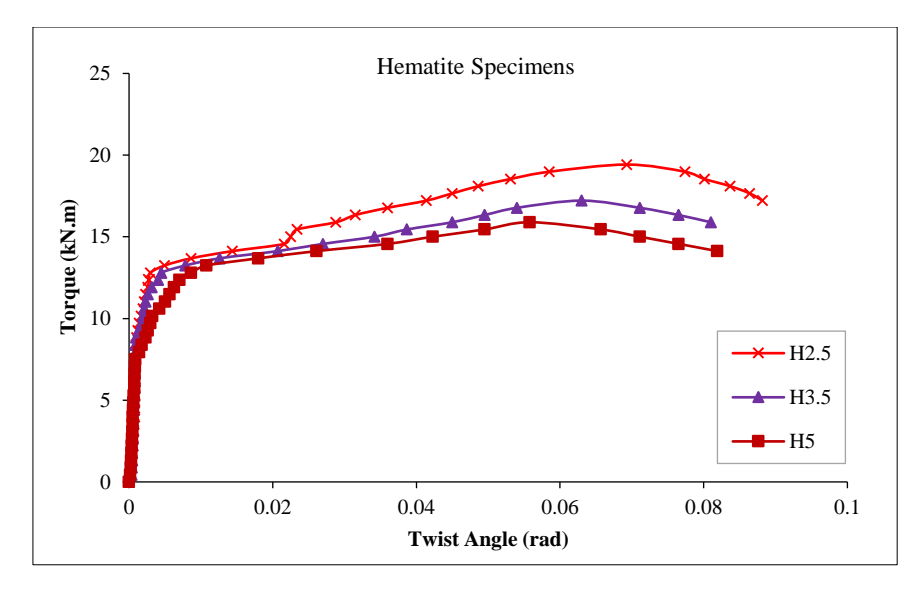


Figure 13. Relationship of Torque-Twist Angle (Hematite Ratio Beyond 2.5%)

Crack Patterns and Modes of Failure: Steel fibers play a significant role in crack development, depending on their distribution within the concrete mix, particularly during the post-cracking stage. The steel fibers act as bridges across crack paths, helping to prevent crack propagation as the load increases [18]. For the specimens in the first stage, it was observed that the initial cracks appeared as inclined cracks on the top and sides of the specimens at the loads listed in Table 5, with angles of approximately  $(43^{\circ} \pm 5)$ . As the load continued to increase, one or more distinct inclined cracks propagated and developed into spiral cracks around the specimen. The crack widths increased progressively until failure occurred, as illustrated in Figure 14.



Figure 14. Failure of First Stage Specimens

As shown in Figure 15, for specimen H0.5, which was designed with a hematite ratio of 0.5%, the crack pattern on the specimen's sides during testing showed one main crack with a few very narrow cracks near the specimen's end, forming at an angle of approximately 41°. With the continued application of load beyond the first crack load until failure, the inclined cracks propagated and widened compared to the initial crack, forming at an angle of about 43°.



Figure 15. Failure of Second Stage Specimens

By increasing the hematite ratio up to 2.5%, the torque at which the first crack occurred increased, and the crack width became smaller compared to the control specimen and specimen H0.5. The first cracking torque values were 8.28 kN·m, 9.27 kN·m, 12.36 kN·m, and 13.68 kN·m, with crack angles of approximately  $(44^{\circ} \pm 4^{\circ})$ . The ultimate torque also increased with the rise in hematite ratio up to 2.5%, while both the crack width and the number of cracks decreased as the hematite powder content increased. The ultimate torque values reached 13.68 kN·m, 15.009 kN·m, and 16.77 kN·m, with corresponding crack angles of  $(44^{\circ} \pm 2^{\circ})$ .

As shown in Figure 14, most cracks were initiated near the supports of the specimens. Based on this observation, it can be stated that the critical section for a specimen under pure torsion is located at the support face. This finding aligns with ACI Code 318-08, Section 11.5.2.4 [4], which specifies that the critical section is located near the support at a distance equal to d [10].

#### 4. Conclusions

According to the experimental results of high-strength steel fiber-reinforced concrete with and without hematite powder subjected to pure torsion, the following conclusions can be drawn:

- There is a significant benefit in using steel fibers to increase both the initial cracking and ultimate torsional strength of high-strength concrete beams under pure torsion.
- It was found that adding higher levels of steel fiber results in greater torsional strength compared to beams without steel fibers. The optimal steel fiber ratio that provides the highest torsional strength while maintaining good workability and avoiding implementation issues was determined to be 1.5%.
- It was observed that end-hooked steel fibers produced higher first cracking and ultimate torque than corrugated steel fibers. Using a mixed combination of steel fibers at the same 1.5% ratio yielded the highest torsional strength without any practical difficulties.
- Adding hematite powder as a cement replacement in high-strength steel fiber-reinforced concrete enhanced both the initial cracking and ultimate torsional strength.
- The highest and most effective first cracking and ultimate torsional strength were achieved at a hematite powder ratio of 2.5%. Increasing this ratio beyond 2.5% led to a reduction in the concrete's compressive and tensile strengths, consequently decreasing the initial cracking and ultimate torsional strength.
- In addition to reducing torsional strength when the hematite powder content exceeded 2.5%, the workability of the concrete also decreased.

# 5. Declarations

# **5.1. Author Contributions**

Conceptualization, M.A. and A.C.; methodology, M.A. and A.C.; validation, M.A.; investigation, M.A.; resources, M.A.; data curation, M.A.; writing—original draft preparation, A.C.; writing—review and editing, A.C.; visualization, A.C.; supervision, A.C.; project administration, M.A.; funding acquisition, M.A. All authors have read and agreed to the published version of the manuscript.

# 5.2. Data Availability Statement

The data presented in this study are available in article.

# 5.3. Funding

The authors received no financial support for the research, authorship, and/or publication of this article.

#### 5.4. Acknowledgements

The authors are grateful to the Department of Civil Engineering of University of Basrah, Iraq.

### 5.5. Conflicts of Interest

The authors declare no conflict of interest.

# 6. References

- [1] MacGregor, J. G., Wight, J. K., Teng, S., & Irawan, P. (1997). Reinforced concrete: Mechanics and design. Upper Saddle River, Prentice Hall, Hoboken, United States.
- [2] Ritter, W. (1899). The Hennebique Construction Method. Swiss Construction Journal, 33(7), 59–61.
- [3] Rausch, E. (1929). Design of Reinforced Concrete in Torsion. Technische Hochschule, Berlin, Germany.
- [4] ACI 318-08 (2008) Building Code Requirements for Structural Concrete and Commentary. American Concrete Institute (ACI), Farmington Hills, United States.
- [5] Broo, H. (2008). Shear and torsion in concrete structures. Chalmers University of Technology, Gothenburg, Sweden.
- [6] Bernardo, L. F. A., Andrade, J. M. A., & Pereira-De-Oliveira, L. A. (2013). Reinforced and prestressed concrete hollow beams under torsion. Journal of Civil Engineering and Management, 19(SUPPL.1). doi:10.3846/13923730.2013.801895.
- [7] Amulu, C., & Ezeagu, C. (2017). Experimental and Analytical Comparison of Torsion, Bending Moment and Shear Forces in Reinforced Concrete Beams Using Bs 8110, Euro Code 2 And ACI 318 Provisions. Nigerian Journal of Technology, 36(3), 705–711. doi:10.4314/njt.v36i3.7.

- [8] Mures, J. K., Ahmed, M. A. I., & Chkheiwer, A. H. (2021). Torsional Behavior of High Strength Concrete Members Strengthened by Mixed Steel Fibers. Journal of Engineering, 2021, 1–8. doi:10.1155/2021/5539623.
- [9] Nazari, A., Riahi, S., Riahi, S., Shamekhi, S. F., & Khademno, A. (2010). Influence of Al2O3 nanoparticles on the compressive strength and workability of blended concrete. Jornal of American Science, 6(5), 6–9.
- [10] Largeau, M. A., Mutuku, R., & Thuo, J. (2018). Effect of Iron Powder (Fe2O3) on Strength, Workability, and Porosity of the Binary Blended Concrete. Open Journal of Civil Engineering, 08(04), 411–425. doi:10.4236/ojce.2018.84029.
- [11] Milasi, S. E., Mostofinejad, D., & Bahmani, H. (2023). Improving the resistance of ultra-high-performance concrete against nuclear radiation: Replacing cement with barite, hematite, and lead powder. Developments in the Built Environment, 15, 100190. doi:10.1016/j.dibe.2023.100190.
- [12] ASTM C150/C150M-24. (2024). Standard Specification for Portland Cement. ASTM International, Pennsylvania, United States. doi:10.1520/C0150\_C0150M-24.
- [13] ASTM C33/C33M-13. (2016). Standard Specification for Concrete Aggregates. ASTM International, Pennsylvania, United States. doi:10.1520/C0033\_C0033M-13.
- [14] ASTM A706/A706M-06. (2017). Standard Specification for Low-Alloy Steel Deformed and Plain Bars for Concrete Reinforcement. ASTM International, Pennsylvania, United States. doi:10.1520/A0706\_A0706M-06.
- [15] Hyperplast PC200. (). High performance concrete superplasciser (Formerly known as Flocrete PC200). Don Construction Products Ltd. Erbil, Iraq.
- [16] MSASA (2017). Technical Datasheet of Silica Fume MegaAdd-MSD. MSASA, Cape Town, South Africa. Available online: https://msasa.co.za/wp-content/uploads/2017/11/MegaAdd-MSD.pdf (accessed on August 2025).
- [17] Abdullah, M. D. (2018). Experimental and Theoretical Behavior of Reinforced Concrete Two Way Slabs Strengthened by Steel Fiber Ferrocement Layers at Tension Zone. Journal of University of Babylon for Engineering Sciences, 26(3), 199–211. doi:10.29196/jub.v26i3.658.
- [18] Kachlakev, D. I., Miller, T. H., Potisuk, T., Yim, S. C., & Chansawat, K. (2001). Finite element modeling of reinforced concrete structures strengthened with FRP laminates. No. FHWA-OR-RD-01-XX, The Oregon Department of Transportation Research, U.S. Department of Transportation, Washington, United States.